JOURNAL OF SOLID STATE CHEMISTRY **23**, 253–263 (1978)

The Crystal Structure of V_4O_7 at 120°K

JEAN-LOUIS HODEAU AND MASSIMO MAREZIO

Laboratoire de Cristallographie, C.N.R.S.—166X, 38042 Grenoble Cedex, France

Received June 19, 1977

The structure of V_4O_7 has been refined at 120°K, which is well below the metal insulator transition (250°K). The room temperature refinement has also been carried out in order to compare it with previous refinements. It seems that charge localization exists already in the metallic phase and becomes almost complete in the insulating phase. Chains of V^{3+} and V^{4+} run parallel to the pseudorutile *c* axis. Charges found for the four independent cations on the two chains 4224 and 3113 are: 3.48–3.35–3.35–3.48, 3.64–3.53–3.53–3.64 at 298°K; 3.11–3.22–3.22–3.11, 3.84–3.83–3.83–3.84 at 200°K; and 3.09–3.24–3.24–3.09, 3.84–3.83–3.83–3.84 at 120°K. In addition there is a short V–V bond between the 1–1 sites in the insulating phase which seems to exist already in the metallic phase, and two short V–V bonds between the 4–2 sites in the insulating phase. The charge localization does not increase below the transition; however, the vanadium cations pair continuously with decreasing temperature below the transition.

V_4O_7 is a member of the homologous series V_nO_{2n-1}. Its structure is related to that of rutile, VO_2, in that it consists of rutile-like blocks, which are infinite in two dimensions and four VO_6-octahedra wide in the third. These blocks are connected along the $(1\bar{2}1)$ plane of the rutile lattice by face-, edge-, and corner-sharing. The resulting structure is triclinic, belongs to space group $A\bar{1}$, and has four independent cation sites. These sites form two independent chains, V(3)–V(1)–V(1)–V(3) and V(4)–V(2)–V(2)–V(4), which run along the pseudorutile *c* axis from one $(1\bar{2}1)$ plane to the next.

In a previous publication Marezio *et al.* (*1*) reported the crystal structure refinement of V_4O_7 above (at 298°K) and below (at 200°K) the metal–insulator transition (250°K). They showed that the metallic phase was characterized by an almost complete disorder of the V^{3+} and V^{4+} cations. The structural refinement at 200°K showed that at the transition these cations are ordered so that chains 3113 have become richer in V^{4+} and chains 4224 richer in V^{3+}. However, the V cations along these chains did not clearly form V–V pairs as the Ti^{3+} cations in the low-temperature insulating phase of Ti_4O_7 (*2*). At that time, in order to have a unified picture of the metal insulator transitions in the Magneli phases, it was argued that the structural refinement of the insulating phase was done only 50°K below the metal insulator transition so that larger changes in bond lengths would be observed at lower temperatures. This conjecture was justified because the transition taking place in V_4O_7 was slightly first order (see, for instance, the variation of the electrical resistivity as a function of temperature, reported in Fig. 1) (*3*) and the NMR data of the insulating phase clearly showed the existence of some singlet cation–cation bonds (*4*). The structural refinements based on X-ray diffraction data above and below the transitions of V_5O_9 (*5*) and Ti_5O_9 (*6*) did not show the existence of cation–cation bonds in the insulating phase of these compounds. It was then assumed that the cation–cation pairs did exist in these crystals,

0022-4596/78/2334-0253 $02.00/0

Printed in Great Britain

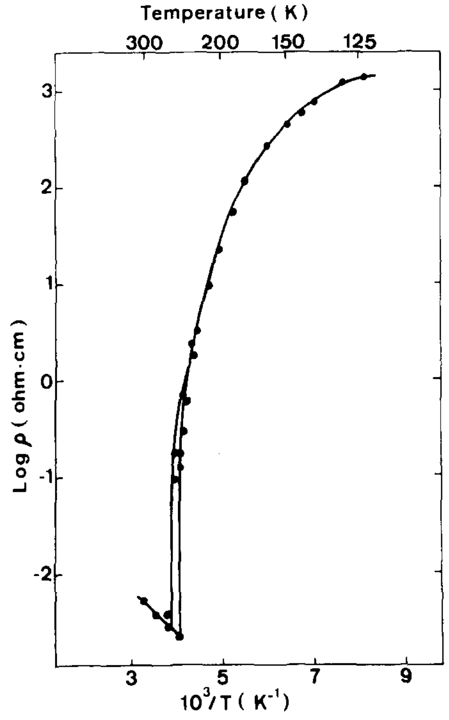

FIG. 1. Electrical resistivity vs reciprocal temperature.

but with no long-range order. Therefore in the Magneli phases the ordered cation–cation bonds have been observed only in the low-temperature insulating phase of Ti_4O_7. Recent results on V-doped Ti_4O_7 showed that 0.6% of V in Ti_4O_7 seems to be enough to suppress the phase with the ordered Ti–Ti pair pattern (*7*).

In order to see whether the V–V pairs did form at lower temperatures, the structural refinement of V_4O_7 was performed at 120°K. This paper reports the results of such a refinement.

Crystal Data

The single crystals of V_4O_7 were grown from a powder sample of V_4O_7 by the vapor transport method. The transport agent was $TeCl_4$. The powder sample was prepared by heating the appropriate mixture of V_2O_3 and V_2O_5 in an evacuated quartz tube at 1000°C for 2 days. For the chemical transport reaction, about 3 g of V_4O_7 was put in a silica tube of 18 mm in diameter and 200 mm in length. Twenty-five milligrams of $TeCl_4$ powder was added, which corresponds to 0.5 mg/cm^3. The tube was evacuated to 10^{-3} mm Hg, sealed off, and put in a horizontal electric furnace. After a back transport, the tube was kept with the hot zone at 1050°C and the cold zone at 1000°C for 5 days.

Precession photographs taken with filtered MoKα radiation showed that the crystals were indeed V_4O_7 and they were untwinned. Vapor-transport crystals of Ti_4O_7 are instead usually twinned (*8*). The intensity measurements were taken with an automatic Philips X-ray diffractometer equipped with a graphite monochromator and AgKα radiation. The low temperatures were attained by blowing a cold stream of nitrogen gas directly on the crystal. A control unit was used to monitor and control the proper temperature and gas flow. The integrated intensities were obtained by the use of ω-scan at room temperature and $\theta/2\theta$ scan technique at low temperature. The background was collected at $\sim\pm 0.6$ degrees off the peak maximum. At room and low temperatures the reflections included in the interval $10^\circ < 2\theta < 60^\circ$ were measured. In order to check the sample orientation and the beam stability three standard reflections (0 6 2), $(\bar{3}\ 0\ 10)$, and $(5\ \bar{6}\ 4)$ were measured about every 2 hr. The specimen was a sphere of radius $R = 0.0054$ cm. Two thousand four hundred and sixty-one and 3534 reflections were measured at 298 and 120°K, respectively; of these, 1245 and 1668 independent reflections well above background were used in the refinements. The intensity of the (2 5 1) and (2 8 4) reflections which are very sensitive to the temperature variation and have an abrupt change at the transition are shown in Fig. 2. These two reflections were used as indicators of the transition temperature. The Lorentz, polarization, and absorption corrections ($\mu R = 0.227$) were applied in order to convert the integrated intensities into structure factors.

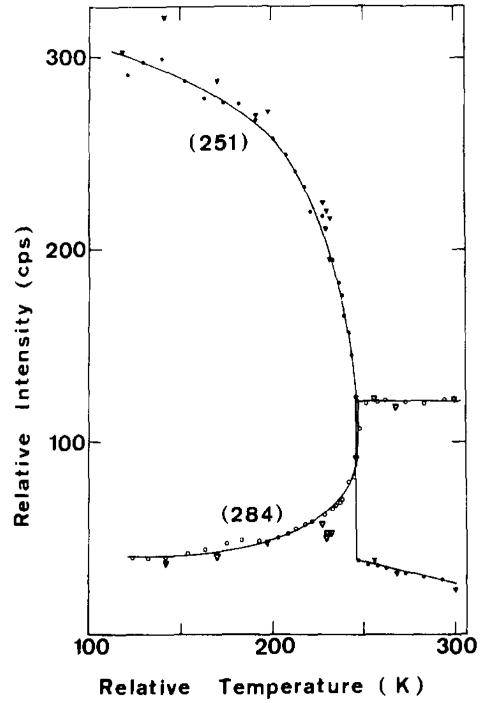

FIG. 2. Net intensities of the (251) and (284) reflections of V_4O_7 single crystal vs relative temperature. The circles are from Ref. (*1*), the triangles are new values.

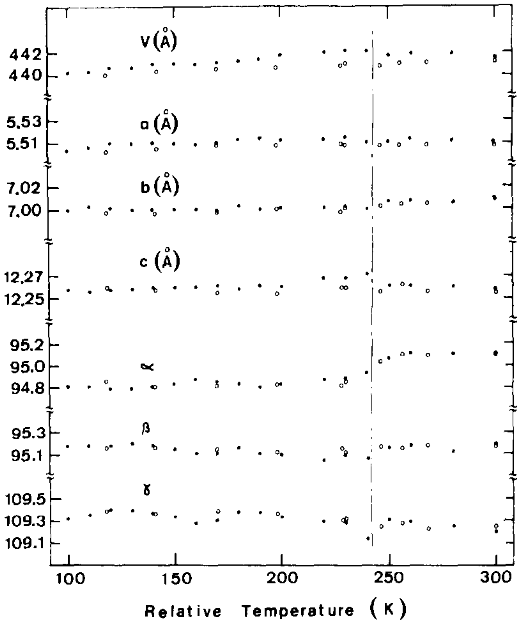

FIG. 3. Lattice parameters and volume vs temperature. The black points are from Ref. (*1*), the circles are new values as determined from a V_4O_7 crystal.

Refinements

The least-squares refinement of the lattice parameters for each temperature was carried out with the PARAM program on the θ angle of 22 well-resolved reflections chosen in the region where a complete α_1/α_2 separation occurred. The zero of the θ circle was determined by measuring for each reflection the θ and the $-\theta$ values. The final parameters are plotted vs temperature in Fig. 3. The points obtained from the earlier publication (*1*), scaled appropriately, are also shown. The values of the lattice parameters at 298 and 120°K which were used for the structural refinements and the calculation of the interatomic distances are given in Table I.

TABLE I

LATTICE PARAMETERS AND UNIT CELL VOLUME USED FOR STRUCTURAL REFINEMENT

	298°K	120°K
a	5.509(1) Å	5.503(1) Å
b	7.008(2) Å	6.997(2) Å
c	12.256(2) Å	12.256(2) Å
α	95.10(2)°	94.86(2)°
β	95.17(1)°	95.17(1)°
γ	109.25(2)°	109.39(1)°
V	441.33 Å^3	440.12 Å^3

The structure was refined with the assumption that the space group was $A\bar{1}$ which had been confirmed previously (*1*). For both refinements the starting values for the positional and thermal parameters were those reported in Ref. (*1*) for 298 and 200°K. The form factor tables for neutral atoms given by Doyle and Turner (*9*) were used, together with values of f′ and f″ for vanadium for AgKα reported by Cromer and Libermann (*10*). The LINEX refinement program was used. At room temperature during the first cycles of refinement, the scale factor, 33 positional parameters, and 11 isotropic thermal parameters were varied, and the conventional

R and *wR* factors were 0.052 and 0.055, respectively. With the introduction of the anisotropic thermal parameters the *R* factors lowered to $R = 0.037$, $wR = 0.039$. It became evident from the strong reflections that an appreciable secondary extinction effect was present in the crystal. Therefore a few more cycles of refinement were done by varying the isotropic secondary extinction factor. The new *R* factors were $R = 0.023$, $wR = 0.019$. The refinement of the low-temperature data was done by varying directly the scale factor, 33 positional parameters, 66 anisotropic thermal parameters, and the isotropic secondary extinction factor: It gave $R = 0.042$ and $wR = 0.032$. The final positional and thermal parameters for the two temperatures are reported in Tables II and III, respectively. These values along with the lattice parameters given in Table I were used as input to the program BONDLA in order to calculate the interatomic distances and the thermal data with their standard deviations. These values are reported in Tables IV and V along with those of the previous study (*1*) for comparison.

TABLE II

Positional Parameters of V_4O_7 at 298°K and 120°K

		298°K	120°K
V(1)	*x*	0.2146(3)	0.2022(2)
	y	0.1468(3)	0.1404(1)
	z	0.0629(1)	0.06216(7)
V(2)	*x*	0.2230(4)	0.2362(2)
	y	0.6550(3)	0.6540(1)
	z	0.0671(2)	0.06961(8)
V(3)	*x*	0.6822(2)	0.6859(2)
	y	0.4403(2)	0.4406(1)
	z	0.1996(1)	0.19785(7)
V(4)	*x*	0.6874(2)	0.6797(2)
	y	0.9419(2)	0.9401(1)
	z	0.2018(1)	0.19961(8)
O(1)	*x*	0.1005(5)	0.1072(6)
	y	0.8576(4)	0.8538(5)
	z	0.0150(2)	0.0136(3)
O(2)	*x*	0.5864(6)	0.5929(6)
	y	0.7958(5)	0.7927(5)
	z	0.0545(2)	0.0466(3)
O(3)	*x*	0.8549(6)	0.8574(6)
	y	0.4932(4)	0.4935(5)
	z	0.0836(2)	0.0861(3)
O(4)	*x*	0.3271(5)	0.3312(6)
	y	0.4367(4)	0.4349(5)
	z	0.1373(2)	0.1373(3)
O(5)	*x*	0.5257(5)	0.5244(6)
	y	0.1433(4)	0.1453(5)
	z	0.1642(2)	0.1641(3)
O(6)	*x*	0.0309(6)	0.0415(6)
	y	0.0641(4)	0.0663(5)
	z	0.1982(2)	0.1944(3)
O(7)	*x*	0.2955(5)	0.2956(6)
	y	0.7922(4)	0.7931(5)
	z	0.2243(2)	0.2244(3)

Results and Discussion

As can be seen from Tables IV and V, the two structural refinements at room temperature are almost identical. For instance, the average octahedral V–O distances are either identical or differ by 0.001 Å. Since these two refinements have been performed by the use of two different crystals and two different diffractometers, the differences in interatomic distances larger than the standard deviations are therefore significant.

As found in the previous experiment the average V–O distances of each octahedron at room temperature indicate that the V^{4+} and V^{3+} cations are not completely disordered, but the chains comprised of V(1) and V(3), that is, chains 3113, are richer in V^{4+} than chains 4224. On the contrary, these latter chains are richer in V^{3+}. The four average distances are V(1)–O = 1.968 Å, V(3)–O = 1.969 Å as against V(2)–O = 1.980 Å, V(4)–O = 1.983 Å. These values are to be compared with the average V^{4+}–O distance found at room temperature in pure VO_2 (1.924 Å)[1] (*11*) and the

---

[1] This value corresponds to a room temperature V–O average distance in a rutile metallic structure. It has been obtained by extrapolating the high-temperature data to 298°K.

TABLE III

THERMAL PARAMETERS ($\times 10^4$)

		298°K	120°K			298°K	120°K
V(1)	β_{11}	46(3)	31(2)	V(3)	β_{11}	36(3)	26(2)
	β_{22}	25(2)	20(1)		β_{22}	25(2)	20(2)
	β_{33}	6.2(6)	3.6(5)		β_{33}	7.3(5)	4.1(5)
	β_{12}	12(2)	11(1)		β_{12}	9(2)	8(1)
	β_{13}	1(1)	0.9(8)		β_{13}	4(1)	2.5(7)
	β_{23}	1.0(7)	0.2(6)		β_{23}	1.7(7)	0.9(6)
V(2)	β_{11}	45(2)	27(2)	V(4)	β_{11}	44(3)	28(2)
	β_{22}	23(2)	18(2)		β_{22}	25(2)	17(2)
	β_{33}	8.5(5)	5.3(4)		β_{33}	8.6(5)	5.5(5)
	β_{12}	14(2)	8(1)		β_{12}	16(2)	8(1)
	β_{13}	2.5(8)	0.4(7)		β_{13}	4.7(9)	2.3(8)
	β_{23}	1.6(7)	1.7(6)		β_{23}	3.5(7)	1.3(7)
O(1)	β_{11}	61(7)	39(8)	O(4)	β_{11}	56(7)	29(8)
	β_{22}	34(5)	13(6)		β_{22}	18(4)	20(6)
	β_{33}	12(1)	7(2)		β_{33}	9(1)	6(2)
	β_{12}	22(5)	13(5)		β_{12}	15(4)	14(5)
	β_{13}	0(3)	0(4)		β_{13}	1(2)	1(3)
	β_{23}	5(2)	−4(2)		β_{23}	1(2)	−1(2)
O(2)	β_{11}	53(8)	40(8)	O(5)	β_{11}	41(7)	43(8)
	β_{22}	41(5)	24(5)		β_{22}	21(5)	20(5)
	β_{33}	9(1)	6(2)		β_{33}	10(1)	6(2)
	β_{12}	8(5)	13(5)		β_{12}	10(4)	12(5)
	β_{13}	3(3)	4(3)		β_{13}	2(2)	0(3)
	β_{23}	4(2)	1(2)		β_{23}	4(2)	0(3)
O(3)	β_{11}	53(7)	42(8)	O(6)	β_{11}	50(7)	21(7)
	β_{22}	33(5)	31(6)		β_{22}	33(5)	28(6)
	β_{33}	9(1)	5(2)		β_{33}	10(1)	5(2)
	β_{12}	10(5)	6(6)		β_{12}	14(5)	11(5)
	β_{13}	7(3)	4(3)		β_{13}	1(3)	3(3)
	β_{23}	5(2)	2(3)		β_{23}	1(2)	5(2)
O(7)	β_{11}	49(7)	32(8)				
	β_{22}	22(4)	16(5)				
	β_{33}	8(1)	7(2)				
	β_{12}	12(4)	2(5)				
	β_{13}	1(3)	4(3)				
	β_{23}	1(2)	2(2)				

average V^{3+}–O distance found in V_2O_3 (2.010 Å) (*12*), which give 1.967 Å for the $V^{3.5+}$–O distance. This value is quite different from the overall average found in V_4O_7: $V^{3.5+}$–O = 1.975 Å.

The determination of the cationic charge from the average cation–oxygen distances is valid only from a qualitative point of view. In a given compound the average interatomic distances depend mainly upon the coordination number and the cationic charge; however, they depend also upon the distortion of the coordination polyhedron and the physical properties of the compound. This last dependence is well illustrated by the average V–O distances found in the three different phases, *R*, M_2, and *T* of $V_{0.985}Al_{0.015}O_2$ (*13*). Two transitions are observed in the electric

TABLE IV

INTERATOMIC DISTANCES (Å) IN V–OCTAHEDRA[a]

	298°K	298°K[b]	200°K[b]	120°K
V(1)–O(1)	1.895	1.897	1.881	1.880
–O(1)	1.932	1.937	1.923	1.922
–O(2)	1.880	1.883	1.818	1.815
–O(4)	2.021	2.010	2.046	2.047
–O(5)	2.032	2.032	2.065	2.065
–O(6)	2.049	2.042	1.954	1.944
Average	1.968	1.967	1.948	1.946
O(5)–O(6)	2.676	2.674	2.603	2.598
O(5)–O(4)	2.659	2.651	2.620	2.611
O(5)–O(2)	2.798	2.793	2.720	2.711
O(5)–O(1)	2.887	2.885	2.895	2.887
O(1)–O(6)	2.799	2.795	2.772	2.767
O(1)–O(4)	2.936	2.933	2.943	2.943
O(1)–O(2)	2.815	2.824	2.794	2.792
O(1)–O(1)	2.618	2.625	2.693	2.708
O(2)–O(4)	2.906	2.902	2.804	2.792
O(2)–O(1)	2.734	2.736	2.692	2.684
O(6)–O(4)	2.794	2.784	2.736	2.732
O(6)–O(1)	2.688	2.685	2.679	2.682
Average	2.776	2.774	2.746	2.742
Standard deviation	0.103	0.102	0.102	0.102
V(2)–O(1)	1.895	1.895	1.913	1.913
–O(2)	1.946	1.940	1.944	1.939
–O(3)	2.011	2.010	2.051	2.052
–O(3)	1.975	1.970	2.027	2.028
–O(4)	2.033	2.037	2.005	1.995
–O(7)	2.020	2.025	2.013	2.005
Average	1.980	1.980	1.992	1.989
O(7)–O(1)	2.826	2.826	2.827	2.816
O(7)–O(2)	2.736	2.739	2.839	2.842
O(7)–O(3)	2.919	2.918	2.904	2.899
O(7)–O(4)	2.687	2.694	2.715	2.715
O(3)–O(1)	2.737	2.737	2.715	2.700
O(3)–O(2)	2.879	2.872	2.877	2.869
O(3)–O(3)	2.701	2.700	2.735	2.732
O(3)–O(4)	2.942	2.941	2.980	2.983
O(3)–O(1)	2.716	2.713	2.708	2.708
O(3)–O(4)	2.788	2.791	2.802	2.797
O(2)–O(1)	2.855	2.845	2.852	2.844
O(2)–O(4)	2.785	2.790	2.823	2.820
Average	2.798	2.797	2.815	2.810
Standard deviation	0.086	0.084	0.085	0.086
V(3)–O(5)	2.125	2.125	2.149	2.151
–O(6)	1.937	1.938	1.922	1.924
–O(7)	1.979	1.979	1.988	1.986
–O(5)	1.964	1.960	1.956	1.949
–O(4)	2.027	2.027	2.017	2.012
–O(3)	1.781	1.783	1.733	1.730
Average	1.969	1.969	1.961	1.959

TABLE IV—*Continued*

	298°K	298°K[b]	200°K[b]	120°K
O(6)–O(5)	2.676	2.674	2.603	2.598
O(6)–O(7)	2.776	2.776	2.751	2.746
O(6)–O(5)	2.893	2.893	2.875	2.874
O(6)–O(3)	2.786	2.794	2.791	2.793
O(4)–O(5)	2.661	2.657	2.653	2.655
O(4)–O(7)	2.646	2.649	2.642	2.636
O(4)–O(5)	2.659	2.651	2.620	2.611
O(4)–O(3)	2.946	2.947	2.928	2.922
O(5)–O(7)	2.577	2.581	2.581	2.573
O(5)–O(5)	2.563	2.559	2.550	2.548
O(3)–O(7)	3.006	3.003	2.983	2.989
O(3)–O(5)	2.847	2.849	2.831	2.821
Average	2.753	2.753	2.734	2.731
Standard deviation	0.146	0.146	0.146	0.148
V(4)–O(4)	2.097	2.098	2.122	2.127
–O(2)	1.932	1.937	2.000	1.999
–O(7)	1.968	1.967	1.974	1.982
–O(7)	2.123	2.125	2.100	2.085
–O(6)	1.809	1.810	1.898	1.902
–O(5)	1.967	1.967	1.959	1.958
Average	1.983	1.984	2.009	2.009
O(4)–O(7)	2.687	2.694	2.715	2.715
O(4)–O(7)	2.646	2.649	2.642	2.636
O(4)–O(6)	2.944	2.947	3.034	3.036
O(4)–O(5)	2.661	2.657	2.653	2.655
O(2)–O(7)	2.899	2.899	2.961	2.973
O(2)–O(7)	2.736	2.739	2.839	2.842
O(2)–O(6)	2.871	2.874	2.926	2.919
O(2)–O(5)	2.808	2.812	2.892	2.901
O(7)–O(7)	2.552	2.552	2.552	2.555
O(7)–O(5)	2.577	2.581	2.581	2.573
O(6)–O(7)	2.854	2.853	2.897	2.901
O(6)–O(5)	3.014	3.015	3.075	3.072
Average	2.771	2.773	2.814	2.815
Standard deviation	0.149	0.149	0.179	0.181

[a] In this table the standard deviations for all V–O distances are respectively ±0.003, ±0.002, ±0.002, ±0.004 Å at 298°K, 298°K[b], 200°K[b], 120°K and for all O–O distances ±0.004, ±0.002, ±0.003, ±0.005 Å at 298°K, 298°K[b], 200°K[b] and 120°K.

[b] The V–O and O–O distances of these temperatures are from Ref. (*1*).

conductivity and magnetic susceptibility of this compound at 340 and 315°K. The *R* (rutile) metallic phase is stable above 340°K, the M_2 (monoclinic) semiconducting phase is stable between 340 and 315°K, and the *T* (triclinic) semiconducting phase is stable

TABLE V

V–V DISTANCES (Å)[a]

	298°K	298°K[b]	200°K[b]	120°K
V(1)–V(1)e	2.791	2.794	2.687	2.669
–V(3)e	2.967	2.964	3.027	3.029
–V(2)c	3.539	3.539	3.547	3.547
–V(2)c	3.491	3.489	3.532	3.535
–V(2)c	3.467	3.474	3.475	3.477
–V(2)c	3.542	3.535	3.538	3.528
–V(4)c	3.721	3.721	3.716	3.709
–V(4)c	3.461	3.459	3.426	3.417
–V(4)c	3.375	3.378	3.370	3.369
–V(3)er	3.068	3.066	3.089	3.089
–V(4)cr	3.760	3.755	3.805	3.809
V(2)–V(2)e	2.932	2.926	3.024	3.030
–V(4)e	2.929	2.930	2.856	2.834
–V(1)c	3.539	3.539	3.547	3.547
–V(1)c	3.491	3.489	3.532	3.535
–V(1)c	3.467	3.474	3.475	3.477
–V(1)c	3.542	3.535	3.538	3.528
–V(3)c	3.675	3.673	3.617	3.602
–V(3)c	3.485	3.486	3.486	3.484
–V(3)c	3.400	3.397	3.384	3.384
–V(4)er	3.008	3.009	2.990	2.989
–V(3)cr	3.716	3.720	3.737	3.737
V(3)–V(1)e	2.967	2.964	3.027	3.029
–V(2)c	3.675	3.673	3.617	3.602
–V(2)c	3.485	3.486	3.486	3.484
–V(2)c	3.400	3.397	3.384	3.384
–V(4)c	3.505	3.502	3.496	3.492
–V(4)c	3.503	3.506	3.509	3.504
–V(4)fr	2.768	2.768	2.781	2.778
–V(4)cr	3.375	3.374	3.399	3.402
–V(3)er	3.191	3.189	3.222	3.219
–V(1)er	3.068	3.066	3.089	3.089
–V(2)cr	3.716	3.720	3.737	3.737
V(4)–V(2)e	2.929	2.930	2.856	2.834
–V(1)c	3.721	3.721	3.716	3.709
–V(1)c	3.461	3.459	3.426	3.417
–V(1)c	3.375	3.378	3.370	3.369
–V(3)c	3.505	3.502	3.496	3.492
–V(3)c	3.503	3.506	3.509	3.504
–V(3)fr	2.768	2.768	2.781	2.778
–V(3)cr	3.375	3.374	3.399	3.402
–V(4)er	3.201	3.202	3.178	3.166
–V(2)er	3.008	3.009	2.990	2.989
–V(1)cr	3.760	3.755	3.805	3.809

[a] The standard deviations for all interatomic distances in this table are ±0.001 Å except for the 298°K distances where it is ±0.002 Å. The symbols c, e, and f refer to V–V distances across a shared octahedral corner, edge, or face, respectively. Symbol r indicates V–V distances between rutile blocks.

[b] The V–V distances of these temperatures are from Ref. (*1*).

below 315°K. On going from the R, to the M_2, to the T structure, the coordination numbers and the cation charges remain unchanged. Therefore the observed anomalous variation of the average V–O distances (see Table VI) is directly related to the metallic or semiconducting character of the different phases. The octahedral distortion varies slightly from the R to the T structure, however, it increases for one vanadium site while it decreases for the other. There is only one V site in the R structure whereas there are two independent cation sites in both the M_2 and T structures.

Recently Zachariasen (*14*) has proposed an empirical method which allows in an ionic compound to determine the cationic and anionic charges. In his method a bond strength is assigned to each individual bond by the formula: $d = d(1)\ (1-0.171 \ln s)$, where d is the individual interatomic distance, $d(1)$ the distance corresponding to unit bond strength, and s the bond strength. The cationic or anionic charge is obtained by summing over the anions or cations of the coordination polyhedron, respectively. The resulting charge takes into account the polyhedral distortion. By summing the calculated s values for each site over the four independent sites, one obtains 13.74 instead of 14.00, which is the theoretical overall cationic charge for V_4O_7. The discrepancy is due to the uncertainty of the $d(1)$ constant ($d(1) = 1.792$). In Table VII the normalized values are given. It is interesting to note that chains 3113 are found to be richer in V^{4+}, while chains 4224 are richer in V^{3+}. However, the distribution along a single chain is not in agreement with the qualitative distribution obtained from the average V–O distances, and it is not what one would predict from the structural arrangement of the Magneli phases. The face-sharing occurring between the V(3) and V(4) octahedra implies that the environment of these cations is sesquioxide-like and that of the V(1) and V(2) is rutile-like. If any order takes place along a chain, one would expect then that the former sites would be V^{3+} rich and the latter V^{4+} rich. On the contrary, the values shown in Table

TABLE VI[a]

V–O AVERAGE DISTANCES AND EFFECTIVE CHARGES IN THE R, M_2, T_{298}, AND T_{173} OF $V_{0.985}Al_{0.015}O_2$ STRUCTURE

	R_{373}		$M_{2(323)}$	T_{298}	T_{173}
V–O average distances	1.926	V(1)	1.945	1.934	1.946
		V(2)	1.946	1.935	1.921
Effective charge	3.88	V(1)	3.90	3.96	3.78
		V(2)	3.96	4.00	4.17

[a] These values are from Ref. (*13*).

VII indicate that the V(3) and V(4) sites are richer in V^{4+} and the V(1) and V(2) sites are richer in V^{3+}. For instance, along chains 3113 the charges are 3.64–3.53–3.53–3.64 whereas along chains 4224 one obtains 3.48–3.35–3.35–3.48.

At room temperature the four octahedra have different distortions. An index of the distortion of an oxygen octahedron is given by the standard deviation calculated from the average of the 12 O–O distances. The indices are 0.103, 0.085, 0.146, and 0.149 for the V(1), V(2), V(3), and V(4) octahedra, respectively. The V(1) and V(2) octahedra, which share only corners and edges, are less distorted than those around V(3) and V(4), which share corners, edges, and faces. The larger distortion of the V(1) octahedron with respect to that of the V(2) octahedron is due to the short V(1)–V(1) distance across the shared edge.

TABLE VII

NORMALIZED V AND O CHARGES CALCULATED WITH THE ZACHARIASEN FORMULA IN THE O AND V COORDINATION POLYHEDRON, RESPECTIVELY

	298°K	298°K[a]	200°K[a]	120°K
V(1)	3.53	3.53	3.83	3.83
V(2)	3.35	3.36	3.22	3.24
V(3)	3.64	3.64	3.84	3.84
V(4)	3.48	3.47	3.11	3.09
O(1)	2.10	2.09	2.11	2.11
O(2)	2.03	2.02	2.08	2.08
O(3)	2.12	2.12	2.15	2.15
O(4)	1.79	1.80	1.79	1.79
O(5)	1.97	1.98	1.92	1.92
O(6)	2.04	2.05	1.98	1.98
O(7)	1.95	1.94	1.97	1.97

[a] These values are calculated with Ref. (*1*) V–O distances.

The idealized structure of V_4O_7 can be thought of as chains of edge-sharing octahedra along the *c* pseudorutile axis, which are 4 octahedra long and are connected to chains of adjacent blocks either by face sharing in the *ac* pseudorutile plane or edge sharing in the *bc* pseudorutile plane. Figure 4 shows these chains of vanadium octahedra, represented as dots, both in the a_Rc_R and b_Rc_R planes. Along chains 4224 the vanadium atoms are equally spaced, the distances being: V(2)–V(2) = V(2)–V(4) = 2.929 Å. This distance is somewhat shorter than the distance one would expect for localized $V^{3.5+}$ cations. A value of 2.935 Å is found for the V^{4+}–V^{4+} distance across the shared edge in the M_2 phase of $V_{0.985}Al_{0.015}O_2$ (*13*). The same value is obtained if one interpolates between the corresponding Ti^{4+}–Ti^{4+} and Cr^{4+}–Cr^{4+} distances in TiO_2 and CrO_2, respectively. The V^{4+}–V^{4+} separation in metallic VO_2 is 2.85 Å (*11*), which is anomalously short and comparable to the $V^{3.5+}V^{3.5+}$ separation found in chains 4224 of V_4O_7. Chains 3113 are comprised of short [V(1)–V(1) = 2.793 Å] and long [V(1)–V(3) = 2.965 Å] V–V distances. The average V–V distance along chains 3113 is 2.879 Å, which is shorter than the average V–V distance (2.929 Å) of chains 4224. This difference is another qualitative proof that the former chains contain on the average smaller cations than the latter. The short V(1)–V(1)

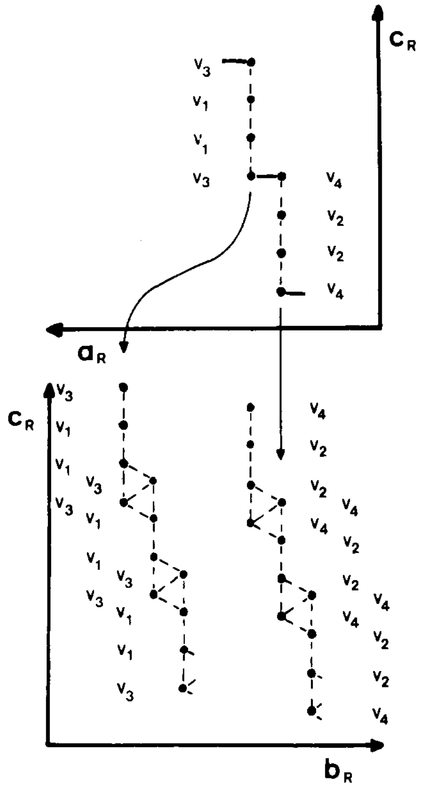

FIG. 4. Idealized projections of the vanadium atoms in V_4O_7 in the rutile cell together with the indices of the vanadium sites. The dashed lines show the edge-sharing contacts where metal–metal bonds might occur. The solid lines are the metal–metal contacts across the shared face of the oxygen octahedra.

separation seems to indicate that already in the metallic state the V(1) cations cannot be considered localized $V^{3.5+}$ cations. They seem to form, instead, covalent bonds between them. In a certain way, the V–V distances pattern found in the metallic phase of V_4O_7 is in between that of metallic rutile and that of the semiconducting M_2 structure found in the $V_{1-x}Cr_xO_2$ (15) and $V_{1-x}Al_xO_2$ systems (*13*). In this latter structure there are two crystallographically independent V-sites, which form two sets of chains parallel to the pseudorutile *c*-axis. On one set all the V cations form V–V covalent bonds with alternating short (2.54 Å) and long (3.26 Å) V–V separations. On the other set the V cations form equally spaced chains, the distance being 2.93 Å. The only difference between the M_2 structure and the metallic V_4O_7 is that in the former phase one half of the V cations are paired whereas in the latter only one quarter are paired.

At the transition the V^{4+} and V^{3+} cations order further on the four sites, in fact at 200°K the V(1)–O and V(3)–O average distances have decreased to 1.948 and 1.961 Å, respectively. They were 1.967 and 1.969 Å at room temperature. On the contrary, the V(2)–O and the V(4)–O average distances have increased to 1.992 and 2.009 Å, respectively. At room temperature they were 1.980 and 1.983 Å. At 120°K these distances decrease slightly (with the exception of the V(4)–O distance which remains the same). This decrease is probably due to the thermal contraction. In every case the decrease in distances is within the corresponding standard deviation. These results seem to indicate that the charge ordering takes place only at the transition and does not increase with decreasing temperature. The calculated *s* charges given in Table VII show that a constant charge of 3.83+ is obtained for the 3113 chains whereas a charge distribution such as 3.09–3.24–3.24–3.09 is obtained for the chains 4224. This corresponds to 83% of the V^{4+} cations on chains 3113 and to the same amount of V^{3+} on chains 4224. On the latter chains the charge is not uniformly distributed as more V^{3+} is concentrated on the V(4) sites, that is, at the end of chains, which is exactly the opposite of the charge distribution found in the metallic phase along a given chain. The octahedral distortions of the V(1), V(2), and V(3) sites remain constant from room temperature to 120°K, whereas that of the V(4) sites increases from 0.149 at room temperature to 0.179 at 200°K and to 0.181 at 120°K. This is probably due to the pairing occurring at the transition between V(2) and V(4). Why the pairing distorts only the V(4) octahedron is not possible to explain.

At the transition the $V(1)^{3.53+}$–$V(1)^{3.53+}$ separation, which is already short in the metallic phase decreases from 2.793 Å at room temperature to 2.687 Å at 200°K and to 2.669 Å at 120°K, whereas the effective charge has increased to 3.83+. The V(1)–V(3) increases from 2.965 Å at room temperature to 3.027 Å at 200°K and then remains almost constant as the value increases only to 3.029 Å at 120°K. Therefore in chains 3113 the pairing of the V(1) cations below the transition increases with decreasing temperature. The value of 2.669 Å at 120°K for the $V(1)^{3.83+}$–$V(1)^{3.83+}$ bonds is comparable to the short V^{4+}–V^{4+} covalent bonds (2.62 Å) found in the insulating phase of pure VO_2 (*16*).

At the metal–insulator transition the cation pairing occurs also along chains 4224. In the metallic phase the four cations are equidistant whereas at 200°K the V(2)–V(2) distance increases to 3.024 Å from 2.929 at room temperature while the V(2)–V(4) distance decreases to 2.856 Å. At 120°K these values further increase (3.030 Å) and decrease (2.834 Å), respectively. If one takes into account that below the transition the V(2) and V(4) cations have an average effective charge of ~3.17+, the V(2)–V(4) distance becomes sufficiently short as to indicate that in the insulating phase chains 4224 do contain two V–V covalent bonds. Since the decrease of the V(1)–V(1) and V(2)–V(4) distances between 200°K and 120°K is much larger than that due to thermal contraction, the speculation that below the transition the cations pair continuously with decreasing temperature seems to be a reasonable one.

Conclusion

The metallic phase of V_4O_7 at room temperature is not comprised of localized V^{3+} and V^{4+} cations completely disordered over the four independent cation sites. The structural refinement shows a partial order by chain, in fact chains 3113 contain 58% of the V^{4+} cations and chains 4224 the same amount of the V^{3+} cations. Furthermore, in each chain the V^{4+} cations are segregated more on the V(3) and V(4) sites, while the V^{3+} ones are segregated on the V(1) and V(2) sites. This distribution along a given chain is not in agreement with the concept of the structure of a Magneli phase, where the cation sites inside a block have an environment more rutile-like than the cation sites at the end of a block. The Zachariasen empirical formula gives the following charge distribution: V(1) = 3.53, V(2) = 3.35, V(3) = 3.64, and V(4) = 3.48. Along chains 4224 the V cations are equidistant, while along chains 3113 there are two long distances (V(3)–V(1) = 2.965 Å) and a short one (V(1)–V(1) = 2.793 Å). This shorter distance seems to indicate that the V(1) cations cannot be considered delocalized $V^{3.5+}$ cations.

The insulating phase is characterized by an order of the V^{3+} and V^{4+} cations over the four cation sites and by the cations pairing along the *c* pseudorutile axis. Since the structural refinements have been done far from the transition it is not possible to know what happens exactly at the transition; however, it seems that the charge ordering takes place at the transition and then remains constant with decreasing temperature, whereas the cation pairing continues to take place below the transition. Chains 3113 have become richer in V^{4+} and each cation of these chains has an effective charge of 3.83+. On the contrary chains 4224 have become richer in V^{3+} and the charge is not uniformly distributed along the chain. The V(2) and the V(4) cations have an effective charge of 3.24+ and 3.09+, respectively.

The bonding pattern of the insulating phase is such that the 3113 chains contain one pair between the two V(1) and the relative distance decreases from 2.793 Å at room temperature to 2.687 Å at 200°K and to 2.669 Å at 120°K. The 4224 chains contain two pairs [V(4)–V(2) and V(2)–V(4)]. The short distance is 2.834 Å at 120°K whereas it is 2.929 Å at room temperature.

References

1. M. Marezio, D. B. McWhan, P. D. Dernier, and J. P. Remeika, *J. Solid State Chem.* **6**, 419 (1973).
2. M. Marezio, D. B. McWhan, P. D. Dernier, and J. P. Remeika, *J. Solid State Chem.* **6**, 213 (1973).
3. S. Kachi, K. Kosuge, and O. Okimaka, *J. Solid State Chem.* **6**, 258 (1973).
4. A. C. Gossard, J. P. Remeika, T. M. Rice, H. Yasuoka, K. Kosuge, and S. Kachi, *Phys. Rev. B* **9**, 1230 (1974).
5. M. Marezio, P. D. Dernier, D. B. McWhan, and S. Kachi, *J. Solid State Chem.* **11**, 301 (1974).
6. M. Marezio, D. Tranqui, S. Lakkis, and C. Schlenker, *Phys. Rev. B* **16**, 2811 (1977).
7. C. Schlenker, S. Lakkis, S. Ahmed, J. L. Hodeau, and M. Marezio, *J. Phys. C* **10**, L151 (1977).
8. J. L. Hodeau, M. Marezio, C. Schlenker, R. Buder, and S. Lakkis, *J. Appl. Crystallogr.* **9**, 391 (1976).
9. P. A. Doyle and P. S. Turner, *Acta Crystallogr. A* **24**, 390 (1968).
10. D. T. Cromer and D. Liberman, *J. Chem. Phys.* **53**, 1891 (1970).
11. D. B. McWhan, M. Marezio, J. P. Remeika, and P. D. Dernier, *Phys. Rev. B* **10**, 490 (1974).
12. P. D. Dernier, *J. Phys. Chem. Solids* **31**, 2569 (1970).
13. M. Ghedira, H. Vincent, and M. Marezio, *J. Solid State Chem,* in press.
14. W. H. Zachariasen, private communication.
15. M. Marezio, D. B. McWhan, J. P. Remeika, and P. D. Dernier, *Phys. Rev. B* **5**, 2541 (1972).
16. J. M. Longo and P. Kierkegaard, *Acta Chem. Scand.* **24**, 420 (1970).